A Series Three-Dimensional Ln_4Cr_4 (Ln = Gd, Tb, Er) Heterometallic Cluster-Based Coordination Polymers Containing Interesting Nanotubes Exhibiting High Magnetic Entropy

Yanzhao Yu[a], Xingxiang Pan[a], Chenhui Cui[a], Ximing Luo[a],Ningfang Li[a], Hua Mei*[a] and Yan Xu*[a] [b]

[a]College of Chemical Engineering, State Key Laboratory of Materials-Oriented Chemical Engineering, Nanjing Tech University, Nanjing 210009, P. R. China

[b]Coordination Chemistry Institute, State Key Laboratory of Coordination Chemistry, Nanjing University, Nanjing 210093, P. R. China

Material and Methods

All the raw chemicals and solvents were purchased from commercial sources and used without further purification. FT-IR spectrums were recorded with Nicolet 470 FT-IR with KBr pellets in the 400 - 4000 cm^{-1} region. Powder X-ray diffraction (PXRD) data was obtained from Bruker AXS X-ray diffractometer using Cu Kα radiation (λ = 1.54056 nm) in the 2ϑ range of 5-50° with a step size of 0.02°. TG-DTA analyses were performed on a NETZSCH TG 209 F3 simultaneous thermal analyzer in flowing N_2 with a heating rate of 10 °C/min. The direct current (dc) magnetic data were measured between 1.8 and 300 K under an applied filed of 1000 Oe. The magnetization measurements were made in fields

of between 0 and 7 T at 1.8-10 K on MPMS-XL7 SQUID magnetometer. Solid-state luminescence properties were acquired by a F-4600 FL spectrophotometer.

Single Crystal X-ray Diffraction

The crystal structure was defined by using the single-crystal X-ray diffraction. Diffraction data for compounds were collected on a Bruker SMART APEX II CCD area-detector diffractometer (Mo *Kα* radiation) at room temperature with *ω*-scan technique. Empirical adsorption correction was utilized using SADABS program.[1] The structure was resolved by direct methods and refined by full-matrix least squares on F^2 using SHELXTL-2018 software.[2] Non-hydrogen atoms were refined anisotropically. Compared with Ln atoms, H atoms of water are very light, and not located. All calculations were performed by using SHELXTL-2018.

Synthetic Discussion

In this work, the nicotinic acid was chose as bridging ligand to construct three novel 3D coordination polymers (**1-Gd, 2-Tb, 3-Er**) with interesting and perfect 1D nanotubes. In order to obtain above compounds, we tried to change the reaction time, reaction temperature and pH value, and finally obtained the crystals by using the synthetic condition described.

During the synthetic process, we found that the formic acid and KBr is important for synthesizing crystals. Although the two raw materials didn't participate the construction of the structure for the three compounds, we can not get the crystals if these two raw materials were lacked. We speculate that these two raw materials act as structural inducer during the crystal structure construction process.[3]

Also, we try to change the lanthanide source to lanthanide chloride, lanthanide nitrate, lanthanide acetate and other lanthanides (Ho, Dy, Eu), unfortunately, no isomorphs or new compounds were gained. The above results indicate that it is advantageous to synthesize these Ln-TM compounds with 3D frameworks with lanthanide oxides as rare earth sources under low pH value.[4]

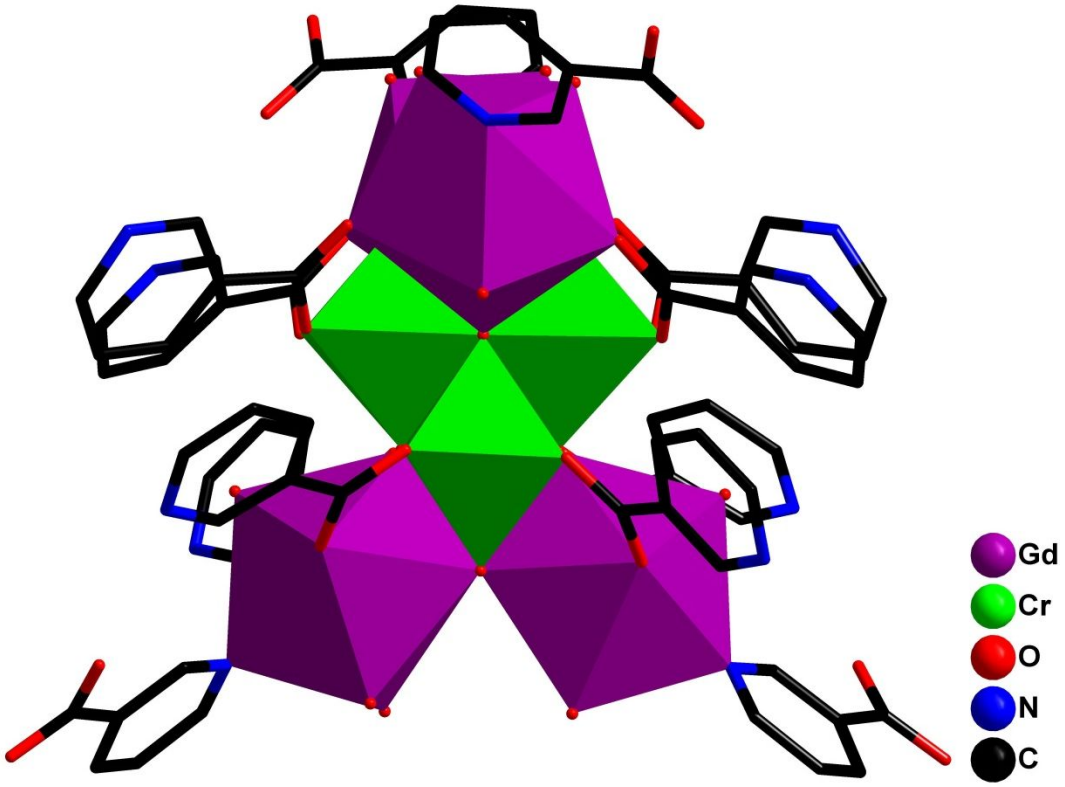

Figure S1. The polyhedron structure of the basic unit for **1-Gd**. Hydrogen atoms were omitted for clarity.

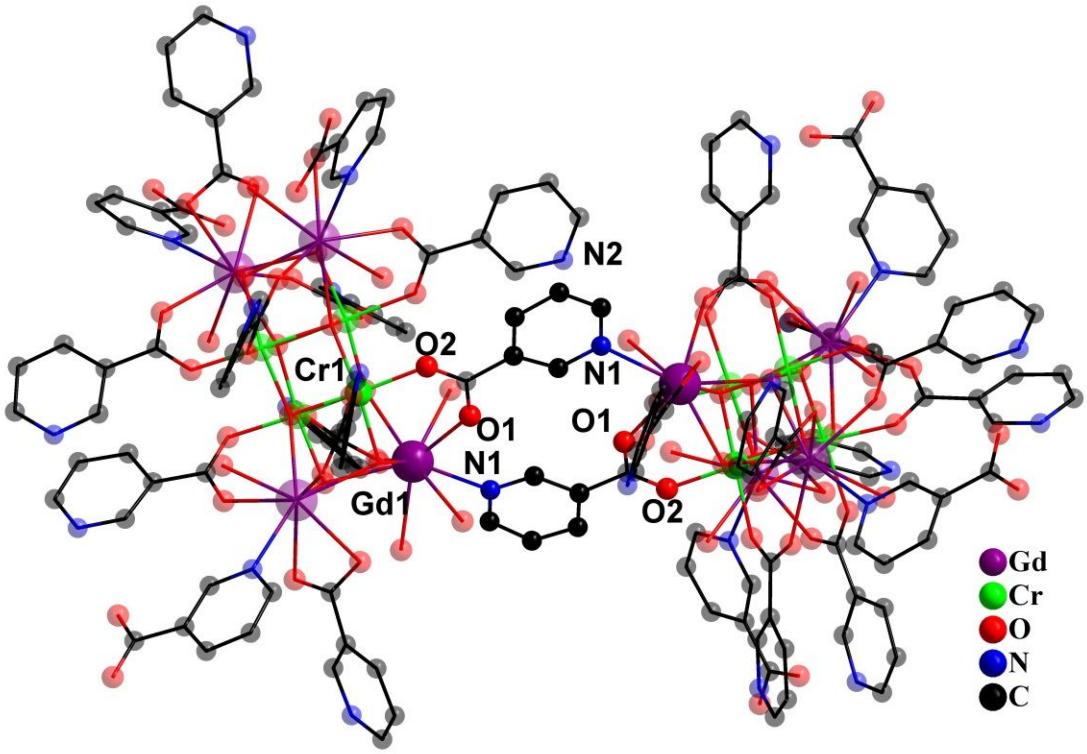

Figure S2. Connection mode of adjacent Gd_4Cr_4 clusters in **1-Gd**. H atoms and lattice water molecules were omitted for clarity.

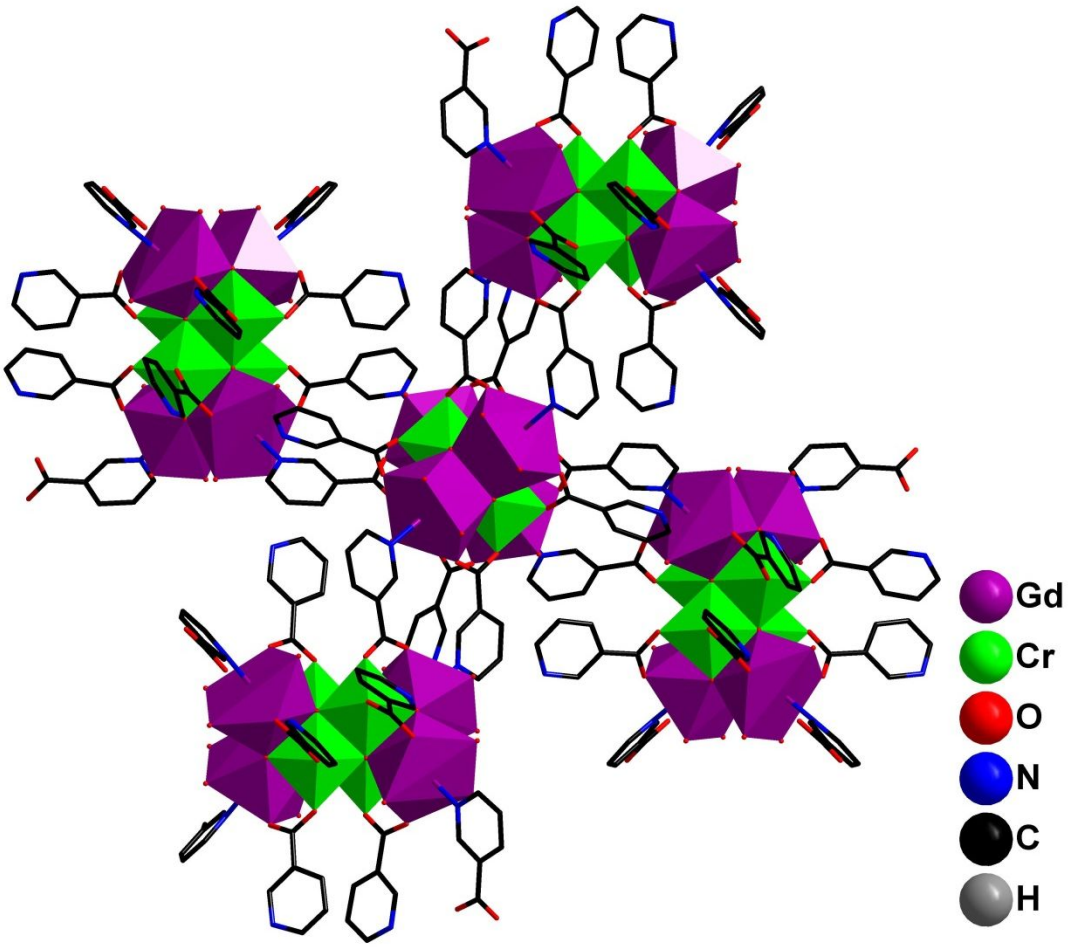

Figure S3. 4-connected mode of Gd_4Cr_4 cluster in **1-Gd**. H atoms and lattice water molecules were omitted for clarity.

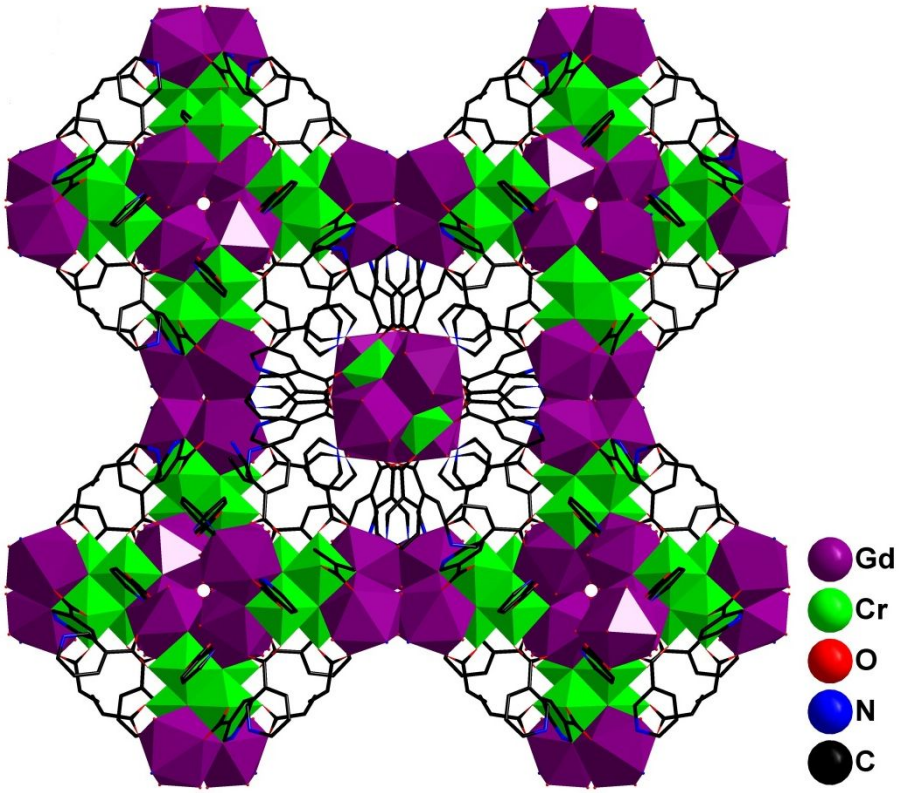

Figure S4. Stick and polyhedral representation of 3D structure of **1-Gd**.

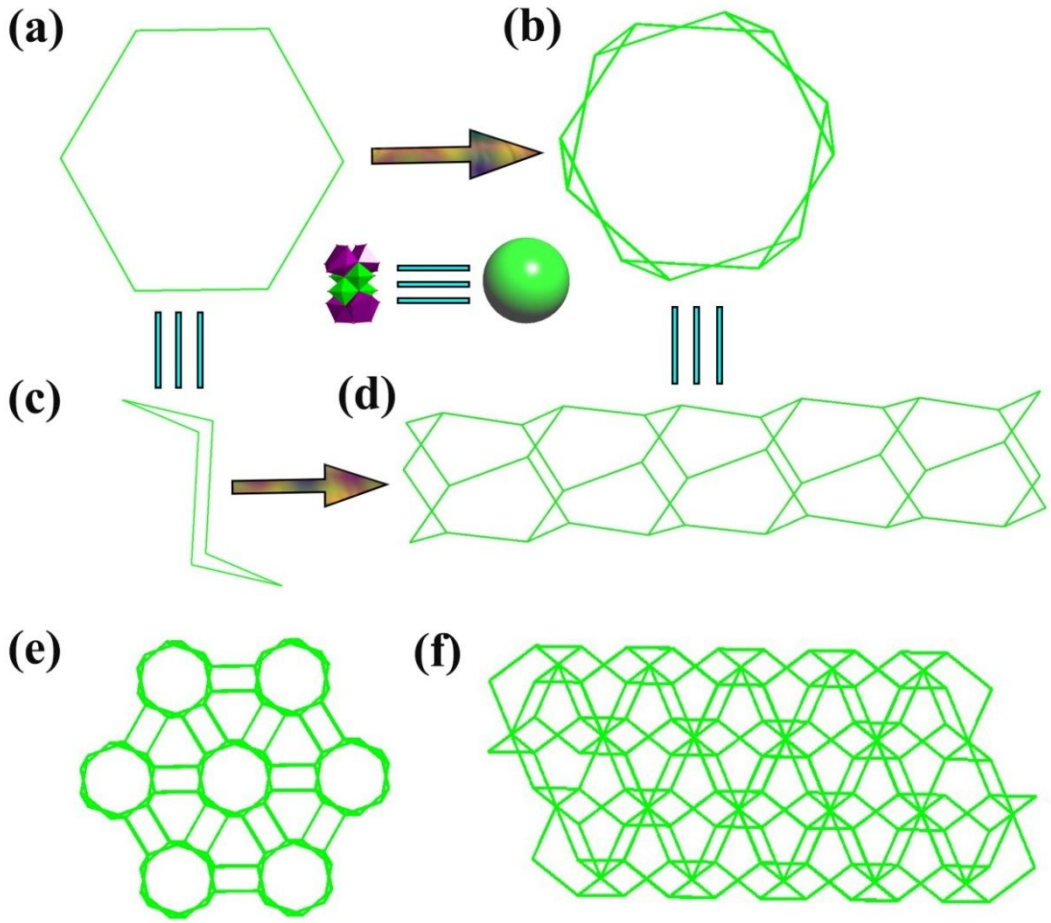

Figure S5. (a) The simplified hexatomic ring; (b) The aperture of 1D tube; (c) The Z-shaped hexatomic ring; (d) The topology network of 1D tube; (e) The topology network of honeycomb-shaped coordination polymer; (f) The topology network of the 3D 1-Gd.

IR Spectra

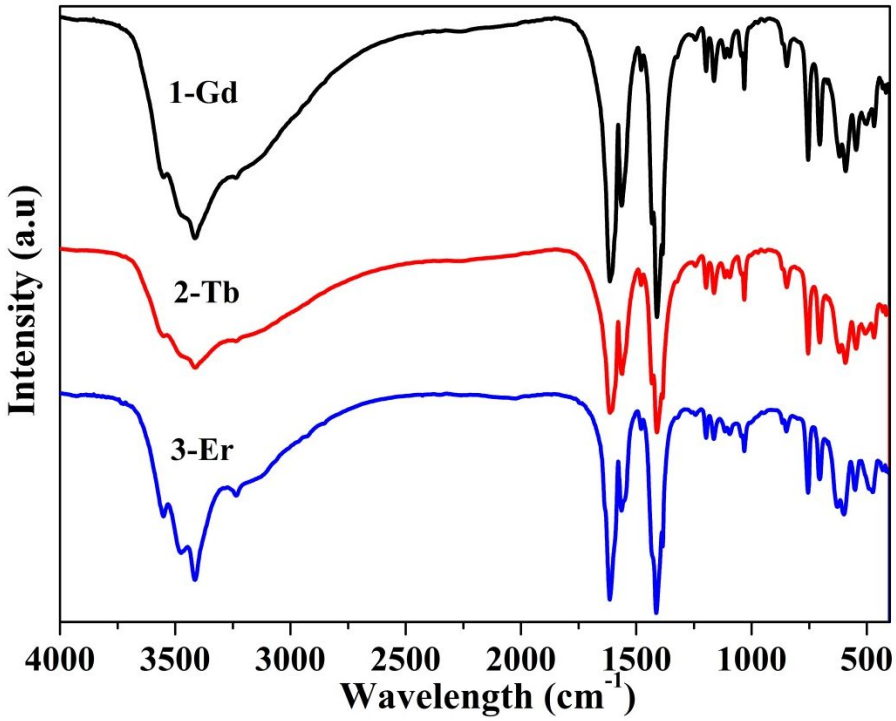

Figure S6. The IR spectrum of Ln_4Cr_4.

The IR spectra of three compounds are similar. As shown in Fig. S5, the broad bands appeared at 3412 cm^{-1} were ascribed to the *v*(-OH). The vibration peaks at 1608 cm^{-1} is characteristic peak of pyridine ring in the nicotinic acid ligand. The peak at 1403 cm^{-1} is assigned to the *v*(C=O). The peaks located between 752–583 cm^{-1} are correspond to *v*(Gd-O) and *v*(Cr-O). The IR spectra implies that the nicotinic acid ligands exist in three compounds, which are well matched with the SCXRD analysis.

Powder X-ray Diffraction (PXRD)

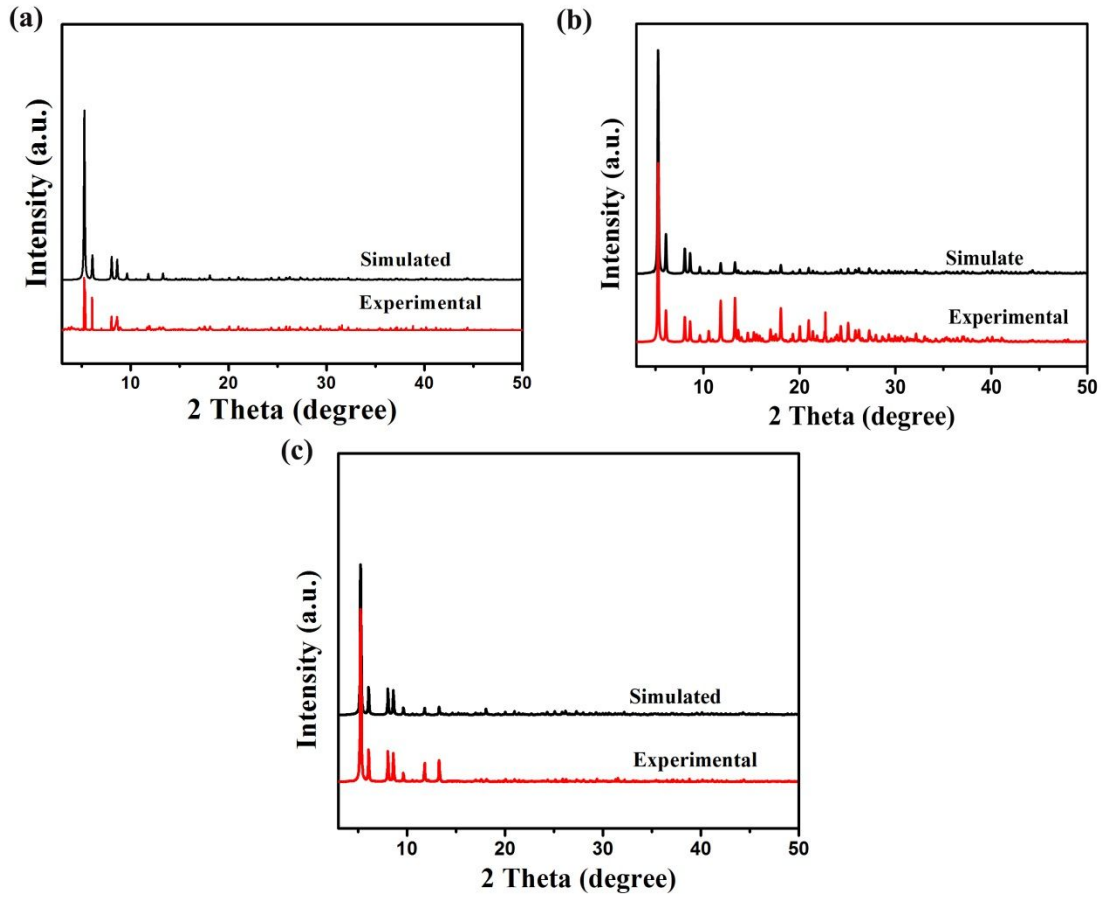

Figure S7. The PXRD spectrum of (a) **1-Gd**; (b) **2-Tb**; (c) **3-Er**.

The PXRD patterns of the three complexes are presented in Fig. S6. The position of main diffraction peaks in the experimental patterns match well with the simulated results from SCXRD, which can imply that the three compounds are pure phase. The difference in reflection intensities may be attributed to the different orientation of the powder samples.

Thermal Gravimetric (TG) Analysis

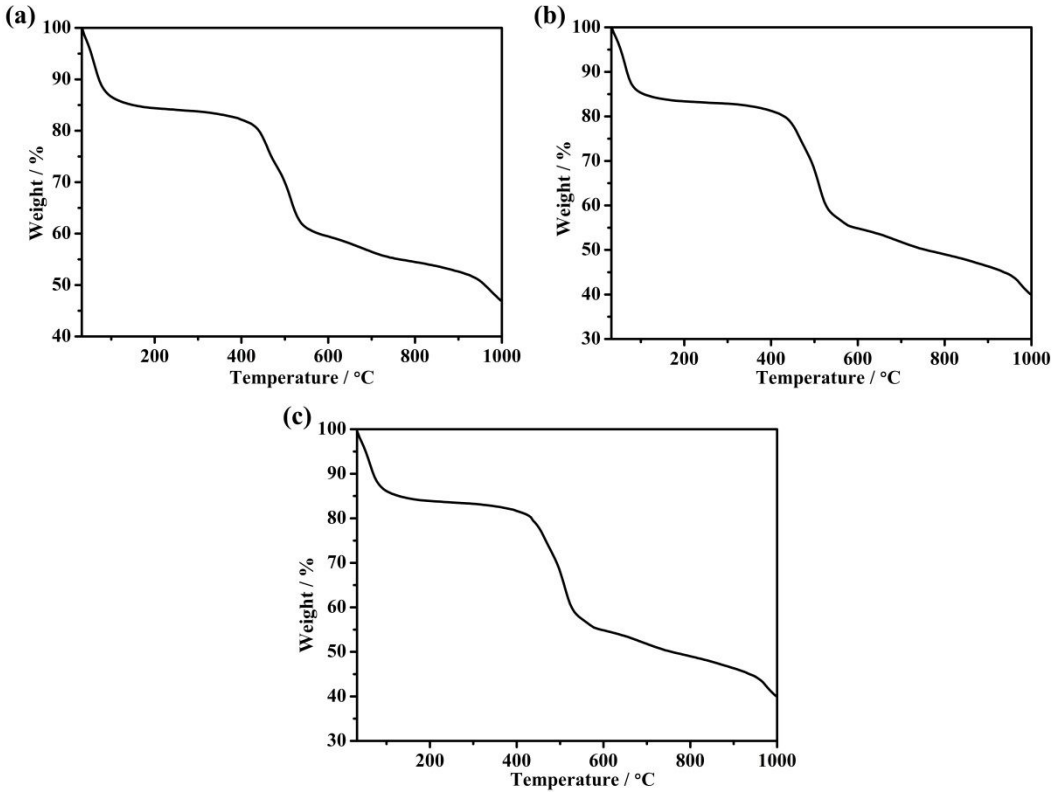

Figure S8. The TG curves for (a) **1-Gd**; (b) **2-Tb**; (c) **3-Er**.

TG analysis was employed to assess the thermal stability of $\mathbf{Ln_4Cr_4}$ from 32 to 1000 °C under N_2 atmosphere. As displayed in Fig. S7, the three compounds exist two similar continuous processes of weight loss. The weight loss of the first process between 32 to 403°C is 17.93, 18.83 and 18.94 %, respectively, (calc. 18.81, 17.73 and 19.50 %), attributing to the loss of lattice water molecules and 12 coordination water molecules in $\mathbf{Ln_4Cr_4}$.The weight loss at 403–1000 °C for three compounds are assigned to the loss of nicotinic acid ligands and the collapsion of the structure of $\mathbf{Ln_4Cr_4}$. The results of TG analysis imply that the three compounds own high thermal stability.

Table S1. Comparision of -ΔS_m^{max} data of the Gd-compound.

compounds	-ΔS_m (J K^{-1} kg^{-1})	ΔH (T)	T (K)	Dimensionality	Ref.
$[Gd_{60}(CO_3)_8(CH_3COO)_{12}(\mu_2\text{-}OH)_{24}(\mu_3\text{-}OH)_{96}(H_2O)_{56}](NO_3)_{15}Br_{12}(CH_3C(OH)_2\text{-}COO)_5\cdot 30CH_3OH\cdot 20CH_3C(OH)_2COOH$	48.0	7	2.0	0D	[5]
$[Co^{II}_9Co^{III}Gd^{III}_{42}(\mu_3\text{-}OH)_{68}(CO_3)_{12}(OAc\text{-})_{30}(H_2O)_{70}](ClO_4)_{24}\cdot 80H_2O$	41.3	7	2.0	0D	[6]
$Ni^{II}_{12}Gd^{III}_{36}(OAc)_{18}(\mu_3\text{-}OH)_{84}(\mu_4\text{-}O)_6\text{-}(H_2O)_{54}(NO_3)Cl_2](NO_3)_6Cl_9\cdot 30H_2O$	36.3	7	3.0	0D	[7]
$[Ni^{II}_2Gd^{III}_2(C(CH_3)_3CO)_4(OAc)_6(H_2O)]\cdot\text{-}2CH_2Cl_2$	34.4	7	4.5	0D	[8]
$[Co^{II}_6Gd^{III}_8(\mu_3\text{-}OH)_8(O_3P^tBu)_6(C(CH_3)_3\text{-}CHO)_{16}\text{-}(H_2O)_2]\cdot 2CH_3CN$	33.0	14	4.0	0D	[9]
$[Ni^{II}_{10}Gd^{III}_5(\mu_3\text{-}OH)_{10}(\mu_5\text{-}NO_3)(C_6H_5N\text{-}O_2)10(C_6H_4N_3O)_{10}](NO_3)_4\cdot 12H_2O\cdot CH_3OH$	27.5	7	4.0	0D	[10]
$[Cr^{III}_4Gd^{III}_4(\mu_3\text{-}O)_4(\mu_4\text{-}O)_4(NA)_8(H_2O)_{12}\text{-}\cdot 13H_2O$	22.1	7	2.5	3D	This work
$[Co^{II}_3Co^{III}_2Gd_3(C_8H_{16}NO_2)_2(\mu_3\text{-}OH)_5(C\text{-}(CH_3)_3CO)_{12}]\cdot 2H_2O$	21.6	7	3.0	0D	[11]
$[Cr^{III}_4Gd^{III}_4(C_6H_4NO_2)_{10}(\mu_3\text{-}OH)_4(\mu_4\text{-}O\text{-})_4(H_2O)_8]\cdot[C_6H_5NO_2]_2\cdot 8H_2O$	18.1	7	3.0	0D	[12]
$[Zn^{II}_8Gd^{III}_4(OH)_8(C_6H_6NO)_8(O_2CCH\text{-}Me_2)_8](ClO_4)_4$	18.0	7	2.0	0D	[13]
$[Ni^{II}_3Gd^{III}(C_6H_6NO)_4(OAc)_5]\cdot H_2O\cdot CH_2\text{-}Cl_2$	17.4	7	4.5	0D	[14]
$[Cu^{II}_5Gd^{III}_2(OAc)_{10}(NO_3)_4(C_{16}H_{17}O_3)_2\text{-}(C_{16}H_{18}O_3)_2]\cdot 4Me_2CO$	15.7	5	2.0	0D	[15]
$[Cu^{II}_{12}Gd^{III}_6(C_{12}H_{10}O_3N_2)_6(OH)_{12}(NO_3\text{-})_7(OAc)_3(H_2O)_{12}](OH)_8\cdot 19H_2O\cdot MeCN$	14	7	4.5	0D	[16]
$[Mn^{III}_6Gd^{III}_2(\mu_3\text{-}OH)_4(\mu_4\text{-}O)(OAc)_4\text{-}(H_2O)_2(C_{16}H_{14}O_3N)_6\cdot NO_3\cdot OH$	10.3	7	6	0D	[17]

OAc = acetate. NA = nicotinic acid. MeCN=acetonitrile. Me=-CH_3. P^tBu=tert-butylphosphonic acid($H_2O_3P^tBu$)

Reference

[1] G. M. Sheldrick, *SADABS, Program for Bruker Area Detector Absorption Correction*, University of Göttingen, Göttingen, Germany, **1997**.

[2] G. M. Sheldrick, SHELXTL Bruker Analytical X-Ray Instruments Inc., Madison, WI, **2018**.

[3] L. Chen, L. Huang, C. L. Wang, J. Fu, D, Zhang, D. R. Zhu, Y. Xu, *J. Coord. Chem*. **2012**, 65, 958-968.

[4]Y. Q. Sun, J. Zhang, Y. M. Chen, G. Y. Yang, *Angew. Chem. Int. Ed*. **2005**, 36, 5964-5967.

[5] X. M. Luo, Z. B. Hu, Q. F. Lin, W. W. Cheng, J. P. Cao, C. H. Cui, H. Mei, Y. Song, Y. Xu. *J. Am. Chem. Soc*. **2018**, 140, 11219−11222.

[6] J. B. Peng, Q. C. Zhang, X. J. Kong, Y. Z. Zheng, Y. P. Ren, L. S. Long, R. B. Huang, L. S. Zheng, Z. Zheng, *J. Am. Chem. Soc.* **2012**, 134, 3314–3317.

[7] J. B. Peng, Q. C. Zhang, X. J. Kong, Y. P. Ren, L. S. Long, R. B. Huang, L. S. Zheng, Z. Zheng, *Angew. Chem. Int. Ed*. **2011**, 50, 10649–10652.

[8] P. Wang, S. Shannigrahi, L. Yakovlev Nikolai, T. S. A. Hor, *Chem. Asian J*. **2013**, 8, 2943–2946.

[9] Y. Z. Zheng, M. Evangelisti, F. Tuna, R.E.P. Winpenny, *J. Am. Chem. Soc.* **2012**, 134, 1057–1065.

[10] G. J. Zhou, W. P. Chen, Y. Yu, L. Qin, T. Han, Y. Z. Zheng, *Inorg. Chem.* **2017**, 56, 12821–12829.

[11] J. A. Sheikh, S. Goswami, S. Konar, *Dalton Trans*. **2014**, 43, 14577–14585.

[12] C. H. Cui, J. P. Cao, X. M. Luo, Q. F. Lin, Y. Xu, *Chem. Eur. J.* **2018**, 24, 15295-15302.

[13] N. Hooper Thomas, J. Schnack, S. Piligkos, M. Evangelisti, K. Brechin Euan, *Angew. Chem. Int. Ed.* **2012**, 51, 4633–4636.

[14] P. Wang, S. Shannigrahi, N. L. Yakovlev, T. S. A. Hor, *Dalton Trans*. **2014**, 43, 182–187.

[15] D. Dermitzaki, O. Bistola, M. Pissas, V. Psycharis, Y. Sanakis, C. P. Raptopoulou, *Polyhedron*. **2018**, 150, 47–53.

[16] J. L. Liu, Y. C. Chen, Q. W. Li, S. Gomez-Coca, D. Aravena, E. Ruiz, W. Q. Lin, J. D. Leng, M. L. Tong, *Chem. Commun*. 2013, 49, 6549–6551.

[17] P. Hu, X. N. Wang, C. G. Jiang, F. Yu, B. Li, G. L. Zhuang, T. Zhang, *Inorg. Chem*. **2018**, 57, 8639–8645.